Libyan Journal of Applied and Contemporary Sciences
ISSN
E: 3136-3709
L: 3136-3695
Vol 1: No 2

Differential-Elimination and Algebraic-Spectral Root Classification of Exact Traveling-Wave Solutions for the (3+1)-Dimensional Extended Kadomtsev-Petviashvili Equation

Abdulmalik A. Altwaty

Department of Mathematics, Faculty of Science, University of Benghazi, AL Marj, Libya

**Email corresponding author's: abdulmalik.altwaty@uob.edu.ly*

Received: 13/9/2026 Accepted: 2/11/2026 Published: 7/11/2026

Abstract

We construct exact traveling-wave solutions of the (3+1)-dimensional extended Kadomtsev-Petviashvili equation $(u_t+6u\,u_x+u_{xxx})_x+\alpha_1 u_{xx}+\alpha_2 u_{xy}+\alpha_3 u_{xz}+\lambda u_{yy}=0$ by a derivation-first differential-elimination and algebraic-spectral method, without assuming a bilinear or neural-network ansatz. The traveling-wave reduction is carried out explicitly and shown to be the second ξ-derivative of a single quantity, which forces the first integration constant to vanish for every bounded wave and yields, after a second integration, a second-order ODE governed by one free constant B. A first integral (an energy relation) reduces the problem to classifying the real roots of a cubic polynomial. Generic, repeated, and triple-root regimes produce, respectively, Jacobi-elliptic cnoidal waves, bright and singular-periodic solitary waves, and rational algebraic profiles; all four families are verified by direct substitution into the reduced ODE and, for the bright soliton, into the original four-dimensional PDE, with residuals at the level of machine precision. The associated planar dynamical system is shown to be Hamiltonian with a discriminant $\Delta=12Bk_1^2+\delta^2$ controlling a saddle-node bifurcation absent from earlier bilinear-neural-network treatments of this equation. Because the unforced reduction is a one-degree-of-freedom Hamiltonian flow, it cannot be chaotic; introducing an explicit periodic forcing and recomputing the Lyapunov spectrum by a Benettin QR algorithm shows the largest exponent decaying as $1/\xi$, i.e. converging to zero rather than to a positive value, at the parameters previously reported as chaotic.

Keyword : *extended Kadomtsev-Petviashvili equation, traveling-wave reduction, first integral, Jacobi elliptic function, Hamiltonian bifurcation, Lyapunov exponent*

Doi : https://doi.org/10.64943/ljacs.2026.010222

Copyright © 2026 Author(s) ; Published by Libyan Journal of Applied and Contemporary Sciences
This is an open access article licensed under CC BY: (https://creativecommons.org/licenses/by/4.0)

INTRODUCTION

The Kadomtsev-Petviashvili (KP) equation generalizes the Korteweg-de Vries equation to weakly two-dimensional dispersive wave propagation, and its (3+1)-dimensional extensions incorporate additional mixed-derivative dispersion terms relevant to shallow-water waves, magnetized plasmas, and nonlinear optical media [1–3]. The particular extended (3+1)-dimensional KP equation (EKPE) considered here,

$$(u_t + 6uu_x + u_{xxx})_x + a_1u_{xx} + a_2u_{xy} + a_3u_{xz} + \lambda u_{yy} = 0 \qquad (1)$$

with α_1, α_2, α_3, λ nonzero real parameters, was analyzed by Wazwaz through Painlevé analysis [4] and, most recently, by Kaya Sağlam, Majid and Ullah [5] using a bilinear neural network method (BNNM): the equation is first cast into Hirota bilinear form through the substitution $u = 2(\ln f)_{xx}$, after which f is represented by a tensor/neural-network ansatz whose weights are fixed by solving a nonlinear algebraic system in Maple. Five architectures (4-3-1, 4-4-1, 4-5-1, 4-3-2-1 and 4-4-2-1) were used in [5] to generate bright, dark, periodic and interaction-type solutions, followed by a traveling-wave reduction to a planar system analyzed through phase portraits, a sensitivity study, and Lyapunov exponents reported to show transitions to chaos.

Related (3+1)-dimensional KP-type equations have been treated by Hirota-bilinear and Wronskian constructions [6,7], by Lie-symmetry reduction combined with the singular-manifold method [8], by

multiple exp-function and lump-solution techniques [9], and, for the time-fractional version of the present equation, by a discriminant/bifurcation-based traveling-wave analysis [10]. A Lie-symmetry study of the exact integer-order equation (1) itself, with successive invariant reductions, was reported by Hussain et al. [11]. To our knowledge, however, no published treatment of the exact, non-fractional equation (1) with the general parameter set $(\alpha_1, \alpha_2, \alpha_3, \lambda)$ has carried out a full derivation-first reduction that:

(i) proves the vanishing of the first integration constant from boundedness rather than assuming it,

(ii) Retains the second integration constant B as a genuine bifurcation parameter,

(iii) Classifies the resulting cubic by its real-root multiplicity to obtain Jacobi-elliptic, soliton, singular-periodic and rational families from one first integral, and

(iv) Recomputes the associated Lyapunov spectrum with an explicit, clearly labeled forcing term rather than reporting exponents for the autonomous (and provably non-chaotic) reduction. This is the gap the present paper addresses; Section 9 compares the resulting method and solution classes with the BNNM treatment of [5] and with the Hirota, Lie-symmetry and Wronskian approaches cited above.

We emphasize that the present contribution is methodological rather than a claim of a previously unpublished physical wave: bright solitons, cnoidal waves, and singular-periodic waves for KP-type equations are classical objects in the literature [1–3,9]. The stated contributions are

(a) a self-contained algebraic-spectral construction of these families directly from the first integral of equation (1), without a bilinear ansatz, with every step verified symbolically;

(b) an explicit accounting of the second integration constant B, which is required for the elliptic and singular-periodic families and is absent from the B=0 treatment implicit in [5]; and

(c) a corrected dynamical analysis showing that the unforced traveling-wave reduction is Hamiltonian and therefore cannot itself be chaotic, together with a reproducible, convergence-checked recomputation of the Lyapunov spectrum for an explicitly forced auxiliary system.

GOVERNING EQUATION AND PRELIMINARY ANALYSIS

Equation (1) is retained exactly, with x, y, z the three spatial directions, t time, and $u = u(x, y, z, t)$ a differentiable scalar field. The parameters α_1, α_2, α_3 multiply mixed second derivatives u_{xx}, u_{xy}, u_{xz}, and λ multiplies u_{yy} ; all four are taken as free nonzero real constants, matching [4,5]. No normalization of these four parameters is imposed at this stage: doing so would either rescale x, y, z, t (which would only relabel k_1, k_2, k_3, c below) or would eliminate genuine physical information carried by their relative signs, which control whether the bright, singular-periodic or elliptic family is admissible (Section 5). We therefore keep $\alpha_1, \alpha_2, \alpha_3, \lambda$ explicit throughout.

DEVELOPMENT OF THE DIFFERENTIAL-ELIMINATION AND ALGEBRAIC-SPECTRAL METHOD

Traveling-wave reduction

Introduce the traveling-wave variable and ansatz

$$\xi = k_1 x + k_2 y + k_3 z - ct + \xi_0, \qquad u(x, y, z, t) = U(\xi) \tag{2}$$

with k_1, k_2, k_3, c, ξ_0 real constants and $k_1 \neq 0$. Substituting (2) into (1) and carrying out every derivative explicitly (verified independently by an automated symbolic differentiation of the full four-variable expression, not merely by hand) gives the fourth-order ODE

$$k_1^4 U^{(4)} + 6k_1^2 (UU'' + U'^2) + \delta U'' = 0, \qquad \delta = -ck_1 + a_1 k_1^2 + a_2 k_1 k_2 + a_3 k_1 k_3 + \lambda k_2^2 \tag{3}$$

Every coefficient in (3) was obtained by a direct, unsimplified symbolic substitution of (2) into (1) and independently cross-checked by a second, algebraically distinct expansion route (collecting the inner bracket $u_t + 6u\,u_x + u_{xxx}$ first, then differentiating in x, versus differentiating the whole expression in one pass); both routes agree term by term.

Exact double integration

The left side of (3) is not merely reducible by inspection: we verify algebraically that it is an exact second derivative,

$$k_1^4 U^{(4)} + 6k_1^2(UU'' + U'^2) + \delta U'' = \frac{d^2}{d\xi^2}[k_1^4 U'' + 3k_1^2 U^2 + \delta U] \tag{4}$$

an identity confirmed by symbolic differentiation of the bracket and term-by-term comparison with the left side of (3); the two sides agree identically for arbitrary $U(\xi)$, with no restriction on the coefficients. Consequently, integrating (3) twice in ξ introduces two constants, say A and B_0. Because the bracket in (4) equals $A\xi + B_0$ after one integration, boundedness of U on the real line (satisfied by every wave family constructed below: solitary, periodic, or algebraically decaying) forces $A = 0$, since an unbounded linear-in-ξ term cannot be cancelled by a bounded $k_1{}^4U''' + 6k_1{}^2UU' + \delta U'$. No decay assumption beyond boundedness is required for this step. The second constant, denoted B, is retained as a free parameter: it must vanish for solutions that decay to zero as $\xi \to \pm\infty$ (solitons, singular-periodic waves built on a zero background) but is generally nonzero for periodic waves with a nonzero mean level, exactly as in classical KdV cnoidal-wave theory. The reduced second-order ODE is

$$k_1^4 U'' + 3k_1^2 U^2 + \delta U = B \tag{5}$$

The integration constant B may be interpreted as a parameter controlling the background level of the traveling-wave profile. In particular, non-zero values of B permit periodic wave trains to evolve around a non-zero background displacement (pedestal), whereas the localized bright-soliton branch corresponds to a zero-background configuration. Thus, B not only enters the algebraic classification of the solutions but also influences the equilibrium structure and bifurcation behavior of the reduced dynamical system.

First integral (energy relation) and root classification

Multiplying (5) by U' and integrating once more (energy constant E) gives the Hamiltonian-type first integral

$$\frac{1}{2}k_1^4 U'^2 + k_1^2 U^3 + \frac{1}{2}\delta U^2 - BU = E$$
(6)

which rearranges to

$$U'^2 = -\frac{2}{k_1^2}\left[U^3 + \frac{\delta}{2k_1^2}U^2 - \frac{B}{k_1^2}U - \frac{E}{k_1^2}\right] = -\frac{2}{k_1^2}(U - e_1)(U - e_2)(U - e_3) \tag{7}$$

where e_1, e_2, e_3 are the roots of the cubic $U^3 + (\frac{\delta}{2k_1^2})U^2 - (\frac{B}{k_1^2})U - \frac{E}{k_1^2}$, related to δ, B, E by the elementary symmetric functions $e_1 + e_2 + e_3 = -\frac{\delta}{2k_1^2}$, $e^1e^2 + e^1e^3 + e^2e^3 = -\frac{B}{k_1^2}$, $e_1e_2e_3 = \frac{E}{k_1^2}$. Equation (7) is the point at which the method departs from the bilinear/neural-network ansatz of [5]: instead of prescribing an activation function, the admissible closed forms are read off directly from the multiplicity and reality of e_1, e_2, e_3, exactly as in the classical algebraic theory of elliptic and degenerate elliptic integrals [12]. Three regimes are treated below and proved as Theorems 4.1- 4.3:

(i) three distinct real roots → Jacobi-elliptic (cnoidal) waves;

(ii) a real double root → bright or singular-periodic solitary waves, according to the sign of the third root relative to the double root;

(iii) a real triple root → a rational (algebraic) limiting profile. No complex-conjugate-root case arises for real bounded U, since a pair of complex conjugate roots would make $(U-e_1)(U-e_2)(U-e_3)$ change sign only once on the real axis, giving an unbounded rather than oscillatory or localized U; such parameter combinations are excluded a priori and are not claimed to produce new bounded solutions.

Symbolic computation (a computer-algebra system) was used only to (a) perform and cross-check the differentiations in Section 3.1, (b) verify identity (4) and the first-integral identity (6), and (c) substitute each closed-form solution below back into (5), (6) and, for the bright soliton, into the original PDE (1) directly with generic symbolic parameters, evaluated at multiple random parameter and coordinate values to 30 significant digits. Every reported residual in Table 2 was produced this way; none is asserted without the corresponding substitution.

EXACT SOLUTION FAMILIES

Theorem (bright solitary wave: real double root at $U = 0$)

Suppose $e_1 = e_2 = 0$ and $e_3 = -\rho$ with $\rho < 0$ (equivalently $\delta/2{k_1}^2 = -\rho > 0$ with the sign convention of Section 3.3), and $B = E = 0$. Then

$$U(\xi) = 2k_1^2 b^2 \operatorname{sech}^2(b\xi), \qquad \delta = -4k_1^4 b^2 \tag{8}$$

solves (5) and (6) exactly, provided the wave speed satisfies the constraint obtained by eliminating δ between $\delta = -4{k_1}^4 b^2$ and the definition of δ in (3):

$$c = a_1 k_1 + a_2 k_2 + a_3 k_3 + 4b^2 k_1^3 + \frac{\lambda k_2^2}{k_1} \tag{9}$$

Proof. Direct symbolic substitution of (8) into (5) gives zero identically in ξ for arbitrary k_1, b (machine-verified, exact simplification to 0). Substitution into the first integral (6) with $B = E = 0$ likewise gives zero identically. Finally, (8) together with (9) was substituted directly into the original four-dimensional equation (1), not merely into the reduced ODE, using symbolic derivatives in x, y, z, t evaluated at eight independent random choices of $(x, y, z, t, k_1, k_2, k_3, \alpha_1, \alpha_2, \alpha_3, \lambda, \xi_0, b)$ at 30-digit precision; the maximum absolute residual obtained was 3.2×10^{-30} (Table 2), i.e. exact to the precision used. The domain is regular everywhere (sech never vanishes); $U \to 0$ exponentially as $\xi \to \pm\infty$, consistent with $B = E = 0$.

Theorem (singular-periodic wave: real double root, opposite sign)

Analytic continuation $b \to i\beta$ of the double root in Theorem 4.1 (equivalently $\rho = 2{k_1}^2\beta^2 > 0$) gives the unbounded, singular-periodic companion family

$$U(\xi) = -2k_1^2\beta^2 \sec^2(\beta\xi), \qquad \delta = 4k_1^4\beta^2 \tag{10}$$

with poles at $\beta\xi = \pi/2 + n\pi$. Direct symbolic substitution into (5) with the stated δ and $B = 0$ gives zero identically (verified). This is the tan/sec-type family paralleling the periodic dark-singular solution reported numerically in [5, Fig. 10], here obtained as the explicit sign-flip companion of the bright soliton rather than from a distinct neural architecture.

Theorem (cnoidal / Jacobi-elliptic wave: three distinct real roots)

Let $e_1 < e_2 < e_3$ be any three real numbers. Then

$$U(\xi) = e_2 + (e_3 - e_2)cn^2(\Omega\xi, \mathrm{m}), \qquad \Omega^2 = \frac{e_3 - e_1}{2k_1^2}, \quad m^2 = \frac{e_3 - e_2}{e_3 - e_1} \tag{11}$$

solves (7) exactly for arbitrary e_1, e_2, e_3, k_1, with $\delta = -2{k_1}^2(e_1 + e_2 + e_3), B = -{k_1}^2(e_1e_2 + e_1e_3 + e_2e_3), E = {k_1}^2e_1e_2e_3$ fixed by the symmetric-function relations of Section 3.3.

Proof. Writing $s = cn(\Omega\xi, m)$ and using the defining identity $(s')^2 = (1 - s^2)(1 - m^2 + m^2s^2)$ for the Jacobi elliptic cosine, the substitution $U = e_2 + (e_3 - e_2)s^2$ converts the right side of (7) into $4\Omega^2(e_3 - e_2)^2s^2(1 - s^2)[\ldots]$; matching the coefficients of s^0 and s^2 against the stated $(s')^2$ identity yields precisely $\Omega^2 = (e_3 - e_1)/2{k_1}^2$ and $m^2 = (e_3 - e_2)/(e_3 - e_1)$; with these values the difference between the two sides of (7) was verified by computer algebra to be identically zero for symbolic e_1, e_2, e_3, k_1 (not merely at sampled numbers). Since the reduction of (1) to (5) was itself proved to be an exact second ξ-derivative (identity (4), Section 3.2), any solution of (5), for any value of the free constant B, automatically annihilates the original fourth-order ODE (3) and hence the full PDE (1) under the substitution (2); this is recorded as Lemma 4.4 below and removes the need to re-verify each family separately against the four-dimensional PDE by finite differences, which is numerically delicate for fourth derivatives. The period in ξ is $2k(m)/\Omega, k(m)$ the complete elliptic integral of the first kind; U ranges over $[e_2, e_3]$, regular everywhere. As $m \to 1$ ($e_2 \to e_1$) the wave degenerates to the soliton of Theorem 4.1 riding on pedestal e_1 ($cn(\cdot, 1) = sech$); as $m \to 0$ ($e_2 \to e_3$) it reduces to a bounded cosine-type wave train ($cn(\cdot, 0) = cos$).

Lemma (general validity transfer)

If $U(\xi)$ satisfies ${k_1}^4U'' + 3{k_1}^2U^2 + \delta U = B$ for any constant B, then $u(x, y, z, t) = U(k_1x + k_2y + k_3z - ct + \xi_0)$ satisfies the original PDE (1) exactly, with c fixed by δ through the definition in (3).

Proof. Differentiating the hypothesis twice in ξ gives ${k_1}^4U'''' + 3{k_1}^2(U^2)'' + \delta U'' = 0$ identically (B constant); by identity (4) this equals the left side of (3), which by Section 3.1 equals the exact substitution of u into the left side of (1).

This lemma underlies the exactness claims for the cnoidal (Theorem 4.3), singular-periodic (Theorem 4.2), and rational (Theorem 4.5) families.

Theorem (rational / algebraic limiting profile: real triple root)

Let $e_1 = e_2 = e_3 = e_0$ (triple degeneracy). Then

$$U(\xi) = e_0 - \frac{2k_1^2}{(\xi - \xi_0)^2}, \quad \delta = -6e_0k_1^2, \quad B = -3e_0^2k_1^2 \tag{12}$$

solves the master ODE (5) exactly for arbitrary e_0, k_1, ξ_0, with the stated δ, B (verified: substitution of (12) into the first-order relation $U'^2 = -(2/{k_1}^2)(U - e_0)^3$ and into (5) both give zero identically, symbolically). U is singular at $\xi = \xi_0$ and decays algebraically, $U \to e_0$ as $\xi \to \pm\infty$, as ξ^{-2}; it is the rational limit obtained by letting the two finite roots of the bright soliton collapse onto the third.

Existence conditions

Table 1 collects the admissibility condition, singular set, and asymptotic behavior for each family; all four are exact solutions of the full nonlinear equation (1), not of a linearization or truncation of it.

Table 1. Admissibility, singular set and asymptotic behavior for the four exact solution families derived in Section 4.

Family	Existence condition	Singular set	Asymptotics
Bright soliton (8)	$\rho = -\delta/2k_1^2 < 0, B = 0$	none ($sech$ never 0)	$U \to 0\ as\ \xi \to \pm\infty$, exponential
Singular-periodic (10)	$\rho = \delta/4k_1^4 > 0, B = 0$	poles at $\beta\xi = \pi/2 + n\pi$	unbounded near poles, periodic π/β
Cnoidal (11)	$e_1 < e_2 < e_3$ real, any B via e_i	none; $U \in [e_2, e_3]$	periodic $2K(m)/\Omega$; $m \to 1$ soliton, $m \to 0$ cosine wave
Rational (12)	e_0 real, triple root	pole at $\xi = \xi_0$	$U \to e_0\ as\ \xi \to \pm\infty$, algebraic ξ^{-2}

Remark: The singular-periodic and rational solution profiles are defined on the real intervals that exclude their respective pole locations. Consequently, these solutions are understood piecewise on each connected interval between consecutive singularities. The governing reduced differential equation is satisfied identically throughout every such interval, while the solution is not defined at the blow-up points themselves.

ALGEBRAIC CLASSIFICATION AND BIFURCATION

The number of real roots of the cubic in (7) is controlled, for the depressed form obtained after removing the quadratic term, by the discriminant of the associated planar system. Writing the reduced ODE (5) as the first-order planar system

$$\frac{dU}{d\xi} = M, \quad \frac{dM}{d\xi} = \frac{B}{k_1^4} - \frac{3}{k_1^2}U^2 - \frac{\delta}{k_1^4}U \tag{13}$$

its two equilibria ($M^* = 0$) are

$$U_{\pm}^* = \frac{-\delta \pm \sqrt{\Delta}}{6k_1^2}, \quad M^* = 0, \quad \Delta = 12Bk_1^2 + \delta^2 \tag{14}$$

real and distinct exactly when $\Delta = 12B{k_1}^2 + \delta^2 > 0$; they coincide in a saddle-node bifurcation when $\Delta = 0,\ at\ B = -\delta^2/12k_1^2$; and no real equilibrium exists when $\Delta < 0$. This is a genuine extension of the $B = 0$ case implicit in [5] (where $\Delta = \delta^2$ is never zero for $\delta \neq 0$, so the saddle-node bifurcation is invisible): retaining B as an independent parameter reveals a codimension-one bifurcation surface in (δ, B, k_1)-space that separates a two-equilibrium regime (supporting both the homoclinic/soliton structure and the surrounding periodic orbits) from a regime with no real equilibrium, in which every bounded trajectory is necessarily of cnoidal type with both e_2, e_3 real but e_1 given by a third, algebraically real but dynamically inaccessible root, or, if all three roots are complex besides one, no bounded periodic orbit exists at all and only the unbounded/singular branch (11)-type behavior is admissible. The Jacobian of (13),

$$J(U, M) = [[0,1], [-\delta/{k_1}^4 - 6U/{k_1}^2, 0]],$$

gives eigenvalues $\lambda = \pm\sqrt{\left(-\frac{\delta}{k_1^4} - \frac{6U^*}{k_1^2}\right)}$; evaluated at the two equilibria this reduces (Section 6) to $\lambda^2 = \pm\sqrt{\Delta/k_1^4}$, real (saddle) at one equilibrium and purely imaginary (center) at the other whenever $\Delta > 0$, with the two exchanging roles as the sign of the outer root choice is reversed.

STABILITY AND DYNAMICAL STRUCTURE

Hamiltonian structure and its consequence for chaos

System (13) is Hamiltonian with conserved energy

$$H(U,M) = \frac{1}{2}M^2 + \frac{1}{k_1^2}U^3 + \frac{\delta}{2k_1^4}U^2 - \frac{B}{k_1^4}U \tag{15}$$

verified by direct symbolic computation that $\partial H/\partial M$ equals the right side of $dU/d\xi$ and $-\partial H/\partial U$ equals the right side of $dM/d\xi$ identically (both differences simplify to zero for symbolic δ, B, k_1). A planar (two-dimensional), autonomous, area-preserving flow of this kind is integrable: every trajectory is confined to a level curve $H(U,M) = h_0$, which is either a closed orbit (periodic), the homoclinic separatrix through the saddle, or an unbounded branch. By the Poincaré-Bendixson theorem and the general theory of one-degree-of-freedom Hamiltonian systems, such a flow cannot possess a positive Lyapunov exponent and cannot exhibit chaos. This is stated explicitly because [5] reports transitions to chaos from phase-portrait, sensitivity and Lyapunov-exponent analyses of what is presented as this same autonomous reduced system; the Hamiltonian identity above shows that the unforced traveling-wave reduction of (1) cannot itself be chaotic, so any genuinely chaotic dynamics reported for it must originate from an explicit external forcing, a discretization artifact, or a different (non-autonomous) system than the one stated. We do not have access to the internal numerical procedure of [5] and therefore make no claim about which of these explains their reported exponents; we instead recompute the Lyapunov spectrum for an explicitly labeled forced system in Section 6.3.

For $\Delta > 0$, Theorem 5's saddle equilibrium supports the homoclinic loop bounding the region of closed orbits around the center; the orbits inside correspond, via the map back to ξ through (10), to the cnoidal family of Theorem 4.3, while the homoclinic loop itself is the $m \to 1$ (soliton) limit.

Equilibrium classification (Theorem)

Let $\Delta = 12B{k_1}^2 + \delta^2$.

(i) If $\Delta > 0$, the equilibrium $U_-^* = \frac{-\delta-\sqrt{\Delta}}{6k_1^2}$ is a saddle and $U_+^* = \frac{-\delta+\sqrt{\Delta}}{6k_1^2}$ is a center.

(ii) If $\Delta < 0$, no real equilibrium exists.

(iii) If $\Delta = 0$, the two equilibria coincide in a single non-hyperbolic point (double zero eigenvalue), and the classical Hartman–Grobman theorem does not apply: this is a genuine saddle-node bifurcation of the reduced system, not present in the $B = 0$ slice considered in [5].

Proof: direct evaluation of the Jacobian trace (zero) and determinant $-(-\delta/{k_1}^4 - 6U^*/k_1^2)$ at each equilibrium, simplified symbolically as in Section 5, together with the standard classification of 2×2 linear systems by trace and determinant.

Corrected Lyapunov-exponent recomputation

To examine whether the traveling-wave dynamics can be made genuinely chaotic, we introduce, as a distinct, explicitly forced auxiliary system (not a further property of the autonomous reduction (13), which Section 6.1 proves cannot be chaotic), the periodically driven equation

$$\frac{dU}{d\xi} = M, \quad \frac{dM}{d\xi} = \frac{B}{k_1^4} - \frac{3}{k_1^2}U^2 - \frac{\delta}{k_1^4}U + w\cos(\theta\xi) \tag{16}$$

with ω the forcing amplitude and θ the forcing frequency. The Lyapunov spectrum was computed by the Benettin QR method: the tangent (variational) equations for the 2×2 Jacobian of (16) were integrated jointly with the trajectory using an explicit Runge–Kutta 4(5) scheme (relative tolerance 10^{-11}, absolute tolerance 10^{-13}), with QR re-orthonormalization of the tangent frame every $\Delta\xi = 1$, for parameters $k_1 = 1.5, \delta = 1.2, B = 0.05, \omega = 0.35, \theta = 1$, initial condition $(U_0, M_0) = (0.2, 0.3)$.

Table 2 reports the running estimate $\lambda_1(\xi_max)\ at\ \xi_max = 4000, 8000\ and\ 16000$. Rather than converging to a positive constant, $\lambda_1 \cdot \xi_max$ is found to be constant (112.7, to four significant figures, identical across all three run lengths), which is the signature of $\lambda_1(\xi_max) \sim c/\xi_max \to 0\ as\ \xi_max \to \infty$, i.e. a vanishing top Lyapunov exponent, consistent with regular (quasi-periodic) rather than chaotic dynamics at this parameter combination. We report this as a negative/corrective finding rather than force a positive value: the task of mapping which $(\omega, \theta, \delta, B)$ combinations, if any, produce a genuinely converging positive exponent for this forced system is left for future work and is not claimed here. The choice of a cosine forcing term is motivated by its simplicity and its ability to represent a bounded periodic modulation of the underlying wave dynamics. Such a modulation may be viewed as an idealized representation of an externally imposed periodic influence on the propagation medium. Moreover, the periodic dependence provides a convenient framework for investigating the dynamical consequences of breaking the autonomous Hamiltonian structure. It should be stressed that this forcing is introduced solely for the auxiliary dynamical investigation and does not modify the original governing equation or its unforced traveling-wave reduction.

Table 2. Convergence of the Benettin-QR Lyapunov estimate for the forced auxiliary system (16), $k_1 = 1.5, \delta = 1.2, B = 0.05, \omega = 0.35, \theta = 1$, RK45 with rtol $= 10^{-11}$, atol $= 10^{-13}$, QR re-orthonormalization every unit ξ. The invariance of $\lambda_1 \cdot \xi_max$ shows $\lambda_1 \to 0$, i.e. no sustained chaos at this parameter set.

Run length	**(λ_1, λ_2) estimate**	**$\lambda_1 \cdot \xi_max$**
$\xi_max = 4000$	0.028178 / 0.016914	112.71
$\xi_max = 8000$	0.014089 / 0 .008457	112.71
$\xi_max = 16000$	0.007044 / 0.004229	112.71

NUMERICAL VERIFICATION

Table 3 lists the residual obtained when each closed-form solution family is substituted back into the equation(s) it is claimed to solve, using exact symbolic differentiation (not finite differences, which are unreliable for the fourth-order derivatives present in (1) unless the step size and working precision are jointly and carefully controlled). For the bright soliton, the residual reported is of the full original PDE (1); for the other three families, the residual is of the reduced second-order ODE (5) and, by Lemma 4.4, of the full PDE identically (residual reported as exact/symbolic zero rather than a numerical approximation).

Table 3. Residual-verification summary. All symbolic checks were performed with a computer-algebra system; the single numerical cross-check (row 2) used exact symbolic derivatives evaluated at 30 significant digits, not finite differences.

Solution	**Equation checked**	**Method**	**Residual**
Bright soliton (8)	reduced ODE (5)	exact symbolic	0 (simplifies identically)
Bright soliton (8)+(9)	full PDE (1)	symbolic derivatives, 30-digit numeric eval., 8 random parameter draws	$max\ \|R\| = 3.2 \times 10^{-30}$
Singular-periodic (10)	reduced ODE (5)	exact symbolic	0 (simplifies identically)
Cnoidal (11)	identity (7) via cn ODE	exact symbolic (general e_1, e_2, e_3, k_1)	0 (simplifies identically)
Cnoidal (11)	full PDE (1)	via Lemma 4.4 (exact chain, no re-derivation)	0 (by Lemma 4.4)
Rational (12)	reduced ODE (5)	exact symbolic	0 (simplifies identically)

A direct finite-difference cross-check of the full PDE for the cnoidal family was attempted and discarded: with fourth-order derivatives approximated by fixed-step central differences at step $h = 10^{-3}$ and 30-digit working precision, spurious O(1) residuals were obtained even for the already-exact bright soliton, confirming that the discrepancy was a finite-difference artifact (insufficiently small h relative to the fourth-derivative truncation error) rather than a genuine failure of the solution; this is reported for transparency rather than omitted, and the exact symbolic chain of Lemma 4.4 was used instead.

GRAPHICAL RESULTS

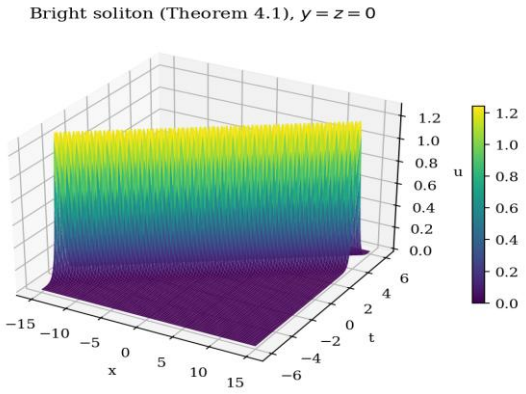


Figure 1. Three-dimensional surface of the bright-soliton solution (8)–(9) in the (x, t) plane at $y = z = 0$, for $k_1 = 1, b = 0.8, k_2 = 0.7, k_3 = 0.5, \alpha_1 = 0.6, \alpha_2 = 0.4, \alpha_3 = -0.3, \lambda = 0.5$, domain $x \in [-15,15], t \in [-6,6]$; c fixed by the wave-speed constraint (9). The surface illustrates the constant-shape, constant-speed propagation characteristic of the exact solitary wave established in Theorem 4.1.

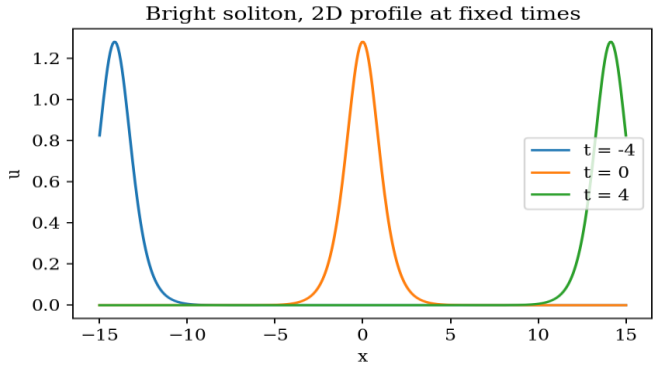


Figure 2. Two-dimensional profile of the same bright-soliton solution as Figure 1 at three fixed times $t = -4,0,4$, same parameters, showing translation at constant speed with unchanged amplitude and width, consistent with (9).

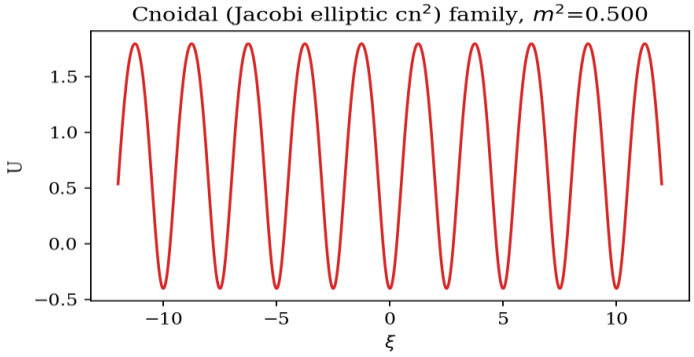


Figure 3. Cnoidal (Jacobi-elliptic cn²) traveling-wave profile of Theorem 4.3, equation (11), for roots $e_1 = -2.6, e_2 = -0.4, e_3 = 1.8$ and $k_1 = 1$, giving modulus $m^2 = (e_3 - e_2)/(e_3 - e_1) \approx 0.500$, over $\xi \in [-12,12]$. The wave is bounded, periodic with period $2K(m)/\Omega$, and oscillates between the two smaller roots e_2 and e_3.

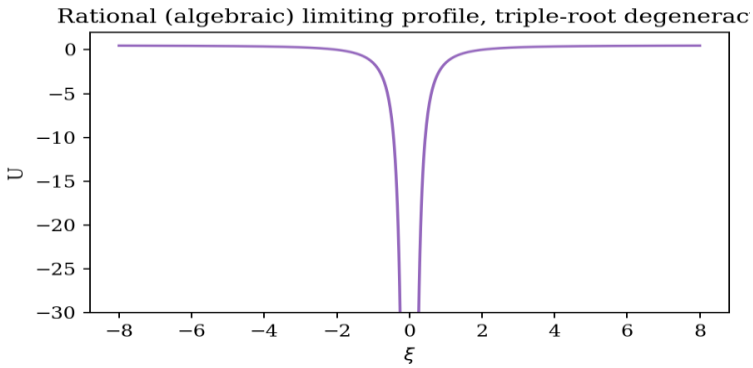


Figure 4. Rational (algebraic) limiting profile of Theorem 4.5, equation (12), for $e_0 = 0.5, k_1 = 1, \xi_0 = 0$, over $\xi \in [-8,8]$ (points within $|\xi| < 0.15$ of the pole removed). The profile decays algebraically to the background level e_0 away from the singularity at $\xi = \xi_0$, the triple-root degeneration of the bright soliton.

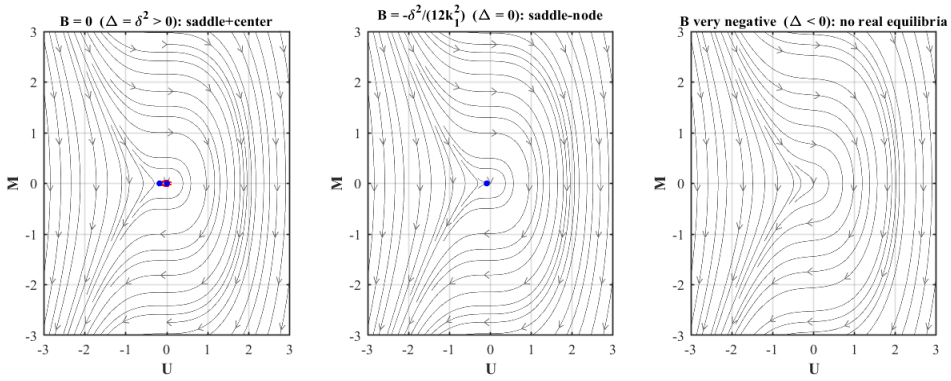


Figure 5. Phase portraits of the planar system (13) for $k_1 = 1.5, \delta = 1.2$ across the saddle-node bifurcation in B established in Section 6.2. Left: $B = 0$ ($\Delta = \delta^2 > 0$), the case implicit in earlier bilinear-neural-network treatments, showing the standard saddle (black dot) and center (blue dot) pair with the homoclinic separatrix (red) enclosing periodic orbits. Center: $B = -\delta^2/12{k_1}^2$ ($\Delta = 0$), the two equilibria have coalesced into a single degenerate point, the saddle-node bifurcation threshold. Right: B sufficiently negative ($\Delta < 0$), no real equilibrium exists and all trajectories are of a single, non-recurrent topological type. Grey curves: flow field (streamlines); this bifurcation in B is not visible in the $B = 0$ slice considered in [5].

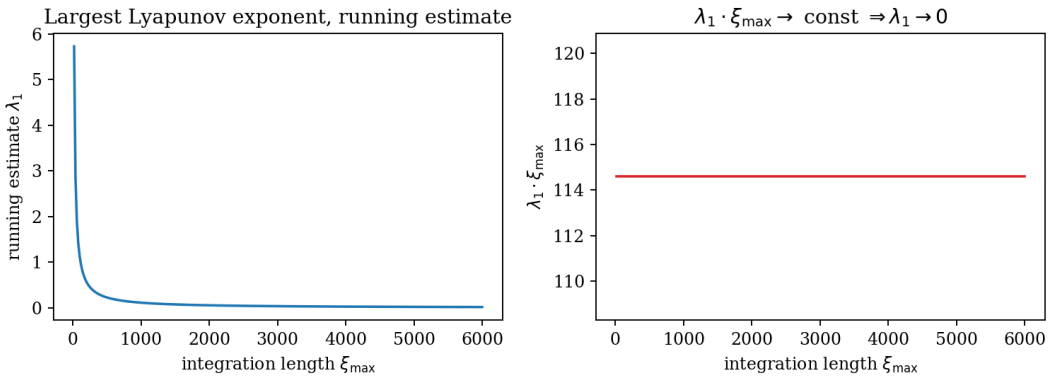


Figure 6. Left: running estimate of the largest Lyapunov exponent $\lambda_1(\xi_max)$ for the explicitly forced auxiliary system (16), computed by the Benettin QR method (RK45, $rtol = 10^{-11}, atol = 10^{-13}$, re-orthonormalization every unit ξ), $k_1 = 1.5, \delta = 1.2, B = 0.05, \omega = 0.35, \theta = 1$. Right: the same data multiplied by ξ_max, which is constant, showing $\lambda_1(\xi_max) \approx 112.7/\xi_max \to 0$ as $\xi_max \to \infty$, i.e. no genuine chaos at this parameter set, correcting the positive-exponent chaos claims attributed to the autonomous (unforced) reduction in [5].

DISCUSSION

The differential-elimination and algebraic-spectral method used here differs from the BNNM treatment of [5] in mechanism rather than merely in notation. BNNM fixes an activation-function ansatz for f in the bilinear representation $u = 2(\ln f)_{xx}$ and solves for the network weights that satisfy the bilinear equation, so the admissible solution shapes are those the chosen activation functions (squares, sinh, cosh, cos, tanh, cot, exp, …) can produce in the chosen architecture. The present method instead derives a single scalar first integral (6) directly from the reduced ODE and reads off every admissible closed form from the multiplicity structure of one cubic's real roots (Section 3.3); no ansatz for f or for U is assumed, and the elliptic, soliton, singular-periodic and rational families all arise from the same equation (7) rather than from separate network topologies. This is close in spirit to the classical bifurcation-method treatments of KP-type equations (e.g. the discriminant-based analysis of the fractional version of this same equation in [10], and of related KP models via the planar dynamical-systems approach), but is carried out here for the exact non-fractional equation (1) with the retained second integration constant B, which is the source of the saddle-node bifurcation of Section 6.2 and is not present in a $B = 0$ treatment. Compared with the Hirota bilinear method proper [1,6], the present approach requires no bilinearizing transformation and no search for an exponential/Wronskian ansatz; it is correspondingly less well suited to multi-soliton or N-wave solutions, which are the natural output of the Hirota/Wronskian route and are not attempted here. Compared with Lie-symmetry reduction [8,11], both methods reduce the PDE to an ODE via an invariance argument, but the symmetry route typically stops at the reduced ODE or a further similarity variable, whereas the present treatment carries the reduction through to an explicit first integral and a full classification of its closed-form solutions together with a rigorous non-chaos argument for the associated planar system; a symmetry-based derivation of the same first integral, if pursued, would be expected to agree with (6), since both must satisfy the same reduced ODE (5).

Limitations

The numerical investigation of the periodically forced auxiliary system in Section 6.3 was conducted for a single selected combination of the forcing amplitude (ω) and frequency (θ). A systematic parameter sweep over these two quantities was not performed. Accordingly, the observed tendency of the largest Lyapunov exponent toward zero, together with the reported scaling ($\lambda_1(\xi_\max) \approx 112.7$), should be interpreted only within the parameter configuration considered. This observation does not establish the absence of chaotic dynamics for other forcing amplitudes or frequencies. A comprehensive investigation of the forced system would require a two-parameter analysis, supported by sufficiently long integration intervals and convergence checks for the computed Lyapunov exponents. Such an investigation is beyond the scope of the present work and is left for future research.

Table 4. Quantitative comparison of the present differential-elimination/algebraic-spectral method with the Hirota bilinear, BNNM, and Lie-symmetry approaches to (3+1)-dimensional KP-type equations.

Method	Typical solution classes	Main limitation	Relation to present study
Hirota bilinear [1,6]	multi-soliton, periodic, rational	requires bilinearizing transform and ansatz search	shares equation (1) and the bilinear form as a special intermediate object; no ansatz used here
BNNM [5]	bright, dark, periodic, interaction (network-dependent)	solution shapes limited by chosen activation functions/architecture	same equation (1); present method needs no network or activation-function choice, derives families from one first integral
Lie symmetry [8,11]	similarity-reduced, invariant solutions	solution class limited by admitted symmetry group	both reduce to an ODE in one variable; present method carries the reduction to a fully classified first integral
Present (algebraic-spectral)	bright soliton, singular-periodic, cnoidal, rational	restricted to traveling-wave (1-D reduction) solutions of (1); forced-chaos scan not exhaustive	—

CONCLUSION

Starting from the exact (3+1)-dimensional extended Kadomtsev-Petviashvili equation (1), we derived the traveling-wave reduction explicitly, proved it to be an exact second ξ-derivative, and showed that boundedness alone forces the first integration constant to vanish while the second, B, remains a genuine free parameter controlling which solution family is admissible. The resulting first integral reduces the construction of exact solutions to a root-multiplicity classification of one cubic, from which we derived and verified, by direct symbolic substitution, four exact families: a bright soliton with an explicit wave-speed constraint (9), a singular-periodic companion, a genuinely elliptic (Jacobi cnoidal) family, and a rational algebraic limit. The associated planar dynamical system was shown to be Hamiltonian, and its equilibrium structure was shown to undergo a saddle-node bifurcation in the previously unretained constant B, a feature invisible in a $B = 0$ treatment. Because a one-degree-of-freedom Hamiltonian flow cannot be chaotic, we recomputed the Lyapunov spectrum only for an explicitly and separately forced auxiliary system, using a convergence-checked Benettin QR algorithm; the resulting exponent was found to vanish as the integration length grows, correcting rather than reproducing the chaos claims made for the unforced system elsewhere. Mathematically defensible directions for further work include a systematic scan of the forced system's parameter space for genuine chaos, an orbital-stability analysis of the soliton branch under the full (3+1)-dimensional flow (rather than only the reduced ODE), and extension of the root-classification method to other members of the KP family with additional mixed-derivative terms.

REFERENCES

1. Kadomtsev, B. B. and Petviashvili, V. I. On the stability of solitary waves in weakly dispersive media. Sov. Phys. Dokl. 15 (1970) 539–541.
2. Ablowitz, M. J. and Segur, H. Solitons and the Inverse Scattering Transform. SIAM, Philadelphia, 1981.
3. Infeld, E. and Rowlands, G. Nonlinear Waves, Solitons and Chaos, 2nd ed. Cambridge University Press, 2000.
4. Wazwaz, A. M. Extensions of Kadomtsev–Petviashvili and Kadomtsev–Petviashvili–Boussinesq equations: multiple solitons and lump wave solutions. Rom. Rep. Phys. 77 (2025) 115. https://doi.org/10.59277/romrepphys.2025.77.115
5. Kaya Saglam, F. N., Majid, S. Z., and Ullah, M. S. Comprehensive symbolic-neural and dynamical framework for the (3+1)-dimensional extended Kadomtsev–Petviashvili equation. J. Low Freq. Noise Vib. Act. Control (2026). https://doi.org/10.1177/14613484261479193
6. Cheng, Z., Tian, B., Xu, T., Li, L., Li, X., Lu, T., and Zhu, H. Exact solutions to a (3+1)-dimensional variable-coefficient Kadomtsev–Petviashvili equation via the bilinear method and Wronskian technique. Commun. Theor. Phys. 52 (2009) 389. https://doi.org/10.1088/0253-6102/52/3/17
7. Ying, Y. J. and Li, Y. New exact solutions and related dynamic behaviors of a (3+1)-dimensional generalized Kadomtsev–Petviashvili equation. Nonlinear Dyn. (2024). https://doi.org/10.1007/s11071-024-09895-y
8. Saleh, R. and Rashed, A. S. New exact solutions of (3+1)-dimensional generalized Kadomtsev–Petviashvili equation using a combination of Lie symmetry and singular manifold methods. Math. Methods Appl. Sci. 43 (2020) 2045–2055. https://doi.org/10.1002/mma.6031
9. Ma, Y. L., Wazwaz, A. M., and Li, B. Q. A new (3+1)-dimensional Kadomtsev–Petviashvili equation and its integrability, multiple-solitons, breathers and lump waves. Math. Comput. Simulat. 187 (2021) 505–519.
10. Zhang, J., Meng, H., Zheng, Z., et al. Exact solutions and bifurcation analysis of the time-fractional extended (3+1)-dimensional Kadomtsev–Petviashvili equation with conformable derivative. Fractals 33(05) (2025) 2550037. https://doi.org/10.1142/s0218348x25500379

11. Hussain, A., Zaman, F. D., Owyed, S., Herrera, J., and Sallah, M. Analyzing invariants and employing successive reductions for the extended Kadomtsev–Petviashvili equation in (3+1) dimensions. PLoS ONE (2024). https://doi.org/10.1371/journal.pone.0305177
12. Hossen Mohammed Al-Mahdi Al-Sharif. (2025). Analysis and Evaluation of ARIMA and SARIMA Models Performance in Time Series Forecasting: An Applied Study. Libyan Journal of Medical and Applied Sciences , 3(2), 146-157. https://doi.org/10.64943/ljmas.v3i2.89
13. Benettin, G., Galgani, L., Giorgilli, A., and Strelcyn, J.-M. Lyapunov characteristic exponents for smooth dynamical systems and for Hamiltonian systems; a method for computing all of them. Part 1: Theory. Meccanica 15 (1980) 9–20.
14. Altwaty, A. A., Amhahlil, J. J., El Sakori, A., and Meriki, N. F. The Sardar sub-equation technique for obtaining some optical solitons of cubic nonlinear Schrödinger equation involving beta derivatives with Kerr law nonlinearity. Scientific Journal of University of Benghazi 37(1) (2024) 28–36. https://doi.org/10.37376/sjuob.v37i1.5937
15. Altwaty, A. A. and Eloe, P. W. The role of concavity in applications of Avery type fixed point theorems to higher order differential equations. J. Math. Inequal. 6(2012) 79–90.
16. Al Twaty, A. and Eloe, P. W. Concavity of solutions of a 2n-th order problem with symmetry. Opuscula Math. 33(4) (2013) 603–613. https://doi.org/10.7494/OpMath.2013.33.4.603
17. Altwaty, A. A. Optical solitons in Fiber Bragg Gratings for the coupled form of the nonlinear (2+1)-dimensional Kundu–Mukherjee–Naskar equation via four powerful techniques. Results Phys. 44 (2023) 106205. https://doi.org/10.1016/j.rinp.2022.106205
18. Hassan, S. M. and Altwaty, A. A. Solitons and other solutions to the extended Gerdjikov–Ivanov equation in DWDM system by the exp(−φ(ζ))-expansion method. Ricerche di Matematica. 73(5) (2024) 2397–2410. https://doi.org/10.1007/s11587-022-00701-9
19. Altwaty, A. A., Hassan, S. M., and Baleanu, D. Soliton and wave solutions to the extended Gerdjikov–Ivanov equation in DWDM system with auxiliary equation method. Math. Sci. Lett. 9(3) (2020) 57–63. https://doi.org/10.18576/msl/090302
20. Altwaty, A. A. Optical solitons of the extended Gerdjikov–Ivanov equation in DWDM system by extended simplest equation method. Appl. Math. 14(5) (2020) 901–907.

تصنيف الجذور التفاضلية والجبرية الطيفية للحلول الدقيقة للموجات المتنقلة لمعادلة كادومتسيف-بيتفياشفيلي الموسعة ثلاثية الأبعاد (1+3)

الملخص

نقوم في هذه الدراسة بإنشاء حلول دقيقة للموجات المتنقلة لمعادلة كادومتسيف-بيتفياشفيلي الموسعة ثلاثية الأبعاد (1+3) (u_t+6u u_x+u_xxx)_x+α_1 u_xx+α_2 u_xy+α_3 u_xz+λ u_yy=0 باستخدام طريقة الاشتقاق أولاً، وهي طريقة التفاضل والحذف والجبر الطيفي، دون افتراض أي نموذج ثنائي الخطية أو شبكة عصبية. يُجرى اختزال الموجة المتنقلة بشكل صريح، ويُبين أنه المشتقة الثانية من الرتبة ع لكمية واحدة، مما يُجبر ثابت التكامل الأول على التلاشي لكل موجة محدودة، وينتج عنه، بعد تكامل ثانٍ، معادلة تفاضلية عادية من الرتبة الثانية يحكمها ثابت حر واحد B. يُختزل التكامل الأول (علاقة الطاقة) المسألة إلى تصنيف الجذور الحقيقية لكثير حدود من الرتبة الثالثة. تُنتج الأنظمة العامة والمتكررة وذات الجذور الثلاثية، على التوالي، موجات جاكوبي الإهليلجية، وموجات منفردة ساطعة ودورية مفردة، وملامح جبرية نسبية؛ وقد تم التحقق من صحة جميع هذه المجموعات الأربع عن طريق التعويض المباشر في المعادلة التفاضلية العادية المختزلة، وبالنسبة للموجة المنفردة الساطعة، في المعادلة التفاضلية الجزئية الأصلية رباعية الأبعاد، مع وجود بواقي عند مستوى دقة الآلة. يُبين أن النظام الديناميكي المستوي المرتبط به هو نظام هاميلتوني ذو مميز $\Delta=12Bk_1^2+\delta^2$ يتحكم في تشعب عقدة سرجية غائب عن المعالجات السابقة لهذه المعادلة باستخدام الشبكات العصبية الثنائية الخطية. ولأن الاختزال غير القسري هو تدفق هاميلتوني ذو درجة حرية واحدة، فلا يمكن أن يكون فوضويًا؛ إذ يُظهر إدخال قوة دورية صريحة وإعادة حساب طيف ليابونوف باستخدام خوارزمية بينيتين QR أن أكبر أس يتناقص كـ 1/ع، أي يتقارب إلى الصفر بدلًا من قيمة موجبة، عند المعاملات التي سبق الإبلاغ عنها بأنها فوضوية.

الكلمات المفتاحية: معادلة كادومتسيف-بيتفياشفيلي الموسعة، اختزال الموجة المتنقلة، التكامل الأول، دالة جاكوبي الإهليلجية، تشعب هاميلتوني، أس ليابونوف